

## Phase Transitions towards Criticality in a Neural System with Adaptive Interactions

Anna Levina,<sup>1,2,\*</sup> J. Michael Herrmann,<sup>1,2,3,†</sup> and Theo Geisel<sup>1,2,‡</sup>

<sup>1</sup>*Bernstein Center for Computational Neuroscience, Bunsenstr a e 10, 37073 G ottingen, Germany*

<sup>2</sup>*Max Planck Institute for Dynamics and Self-Organization, Bunsenstr a e 10, 37073 G ottingen, Germany*

<sup>3</sup>*University of Edinburgh, School of Informatics, IPAB, 10 Crichton Street, Edinburgh EH8 9AB, United Kingdom*

(Received 27 August 2008; published 20 March 2009)

We analytically describe a transition scenario to self-organized criticality (SOC) that is new for physics as well as neuroscience; it combines the criticality of first and second-order phase transitions with a SOC phase. We consider a network of pulse-coupled neurons interacting via dynamical synapses, which exhibit depression and facilitation as found in experiments. We analytically show the coexistence of a SOC phase and a subcritical phase connected by a cusp bifurcation. Switching between the two phases can be triggered by varying the intensity of noisy inputs.

DOI: 10.1103/PhysRevLett.102.118110

PACS numbers: 87.18.Sn, 05.65.+b, 64.60.Ht, 89.75.Fb

The concept of self-organized criticality (SOC) [1] describes a variety of phenomena ranging from plate tectonics [2], the dynamics of granular media [3] and stick-slip motion [4] to neural avalanches [5]. These examples have in common that a marginally stable dynamics is maintained by self-tuning of parameters towards critical values and that the event sizes obey a characteristic power-law distribution. When criticality had been observed also in neural systems [6] a number of studies addressed its functional role: Criticality was shown to bring about optimal computational capabilities [7], optimal transmission [6] and storage of information [8], and sensitivity to sensory stimuli [9].

In analogy to the physical systems mentioned above, the strength of the interaction among the neural units by synaptic connections has been identified as a critical parameter [5]. In real neural systems the connection strengths are not static but depend on the relative timing of the neural activity pulses [10]. Numerical simulations [11] indicated that the dynamics of the synaptic efficiencies may account for the occurrence of SOC in neural systems. While the system with static coupling has a classical critical point [5], we show analytically that the adaptive model attains criticality in an extended region of the parameter space that is bounded by phase transitions. The critical region of the connectivity parameter (at least in the case of a finite network, cf. below) is sandwiched between a sub- and a supercritical regime which also can be reached experimentally by a manipulation of the synaptic strengths. The system exhibits a rich dynamical behavior including a hysteresis between critical and noncritical dynamics, switching of the dynamics in dependence of external inputs, and first- and second-order phase transitions that form a cusp bifurcation. Although presented in the specific context of a neuronal model, this dynamical structure is of more general interest as the first observation of a complex classical bifurcation scenario combined with a SOC phase.

We consider a system of neurons (threshold integrators) that interact by exchanging short pulses of activity. In the neurophysiological interpretation, these action potentials or spikes are transformed into chemical signals that are transmitted across the synaptic cleft in between two neurons. The amount of transmitter emitted at a synaptic terminal depends only on the relative timing of arriving pulses. We denote this amount by  $J_{ij}$  and the fraction that is available for signaling at a given moment by  $u_{ij} \in [0, 1]$ , where  $i$  and  $j$  refer to the pre- and postsynaptic neurons, respectively. We can express the interaction strength by the product  $u_{ij}J_{ij}$ . The state  $h_i \geq 0$  of neuron  $i = 1, \dots, N$  represents the membrane potential and obeys the following equation:

$$\dot{h}_i = \delta_{i,\zeta(t)}I + \frac{1}{N} \sum_{j=1}^N u_{ij}(t_{\text{sp}})J_{ij}(t_{\text{sp}})\delta(t - t_{\text{sp}}^j - \tau_d). \quad (1)$$

By the first term a neuron is selected to receive an external input of strength  $I$ , where  $\delta_{i,\zeta}$  ( $\delta_{i,\zeta} = 1$  if  $i = \zeta$  and  $\delta_{i,\zeta} = 0$  otherwise) is the Kronecker symbol.  $\zeta$  denotes a random process with an event rate  $\tau_s^{-1}$ . We assume that  $I$  scales with the system size as  $I = \frac{I_0}{N}$  for numerical simulation and analysis in the thermodynamical limit. A spike from neuron  $j$  is assumed to affect neuron  $i$  precisely after a delay  $\tau_d$  and enters Eq. (1) via Dirac's delta function ( $\delta(t) = 0$  if  $t \neq 0$  and  $\int \delta(t)dt = 1$ ).

When the membrane potential  $h_i \geq 0$  exceeds a certain threshold  $\theta$  at time  $t_{\text{sp}}^i$  then neuron  $i$  emits a spike. It is then reset by subtracting the threshold  $\theta$ :  $h_i(t_{\text{sp}}^+) = h_i(t_{\text{sp}}) - \theta$ . Synaptic activity also reduces the amount of neurotransmitters such that  $J_{ij}$  is diminished immediately after a spike [12]. In between spikes, the resources recover and  $J_{ij}$  approaches its resting value  $\frac{\alpha}{u_0}$  at a time scale  $\tau_J$ ,

$$\dot{J}_{ij} = \frac{1}{\tau_J} \left( \frac{\alpha}{u_0} - J_{ij} \right) - u_{ij}J_{ij}\delta(t - t_{\text{sp}}^j). \quad (2)$$

There is experimental evidence that the value of  $u_{ij}$  is also subject to an activity-dependent dynamics [12]. By

$$\dot{u}_{ij} = \frac{1}{\tau_u}(u_0 - u_{ij}) + (1 - u_{ij})u_0\delta(t - t_{sp}^i) \quad (3)$$

the effective synaptic strength increases through the activation of silent resources inside the synaptic terminal. Thus, while the dynamics of  $J_{ij}$  has a depressive effect on the neural activity, activity-related changes in  $u_{ij}$  tend to facilitate the neural response. During pauses,  $u_{ij}$  decays with a time scale  $\tau_u$  towards its minimal value  $u_0$ , i.e., the minimal level of activated synaptic resources [12]. The quantity  $\frac{\alpha}{u_0}$  in Eq. (2) is the main parameter of the model which represents the maximum of a synaptic strength of a synapse.

The joint effect of facilitation and depression depends on the time scales  $\tau_u$  and  $\tau_J$  which are assumed to be slow compared to the external input, i.e.,  $\tau_J = \nu_J \tau_s N$ ,  $\tau_u = \nu_u \tau_s N$ , and  $1 < \nu_J, \nu_u \ll N$ . For simplicity we assume  $\nu_J = \nu_u = \nu$ . However, for  $\nu_J \neq \nu_u$  the same qualitative behavior was found in the critical state with accordingly modified values of  $u_0$  and  $\alpha$ .

Each firing event increases the probability that other neurons are activated such that a number of neurons may join the externally triggered activity and create a neural avalanche. Roughly speaking, when the avalanches are large and neurons fire often, synaptic depression is dominant and causes a reduced activity and, therefore, smaller avalanches. On the other hand, sparse firing events lead to almost fully recovered synapses and the facilitation of the synapses becomes essential. The distribution of the number of neurons participating in an avalanche depends on the value of  $\alpha$ . Qualitative changes occur at two critical values  $\alpha_c = 0.533$  and  $\alpha^c = 0.543$  (for the parameters used in Fig. 1, for other parameters cf. Fig. 5). The subcritical regime at small  $\alpha < \alpha_c$  is characterized by a negligible number of avalanches that extend to the size of the system. At large  $\alpha \gg \alpha^c$  many large avalanches occur and the distribution becomes nonmonotonic. In between  $\alpha_c$  and  $\alpha^c$  and for some interval beyond  $\alpha^c$  the system has an approximate power-law distribution for a large volume of initial conditions. Between  $\alpha_c$  and  $\alpha^c$  the subcritical branch persists, cf. Fig. 1. At the boundaries of the interval  $[\alpha_c, \alpha^c]$  the stationary behavior undergoes a sharp transition from subcritical to critical behavior. Along the upper branch the distribution stays critical for a large interval of the parameter  $\alpha$ . The deviation from an ideal power law (Fig. 2) is considerably smaller than in the depressing case [13] and the region where a critical distribution is suggested by the numerics increases with system size (Fig. 2, inset). For static synapses, in contrast, the critical region approaches a single point on the  $\alpha$  axis.

The behavior of the network can be understood by a self-consistency equation that relates the averages of the two main dynamical quantities, namely, the average synaptic strength  $u_{ij}J_{ij}$  and the interspike interval  $\Delta^{\text{isi}}$ . The exist-

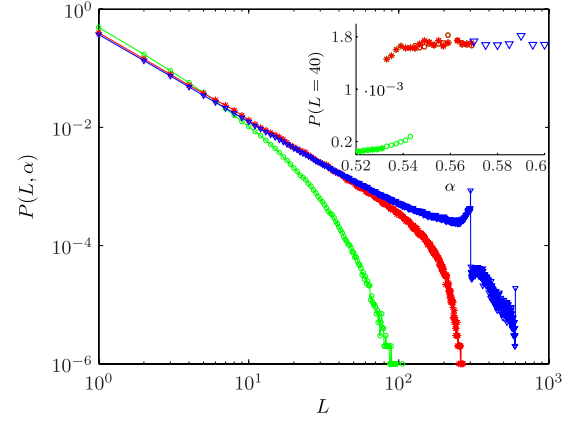


FIG. 1 (color online). Examples of distributions of avalanche sizes in dependence on the interaction parameter  $\alpha$ . Circles: subcritical distribution ( $\alpha = 0.52$ ), stars: critical branch ( $\alpha = 0.56$ ), triangles: supercritical ( $\alpha = 0.59$ ) for  $N = 300$ ,  $\nu = 10$ ,  $u_0 = 0.1$ ,  $I_0 = 7.5$ . Inset: Probability of an avalanche of length  $L = 40$ . Circles are obtained by incrementing  $\alpha$  and stars by decrementing  $\alpha$ .

tence of the averages is implied by the uniform boundedness of  $u_{ij}$  and  $J_{ij}$  and the mixing properties of the network dynamics. The dynamics of  $u_{ij}$  (3) does not depend on  $J_{ij}$ ; therefore, we first establish the dependency of  $u_{ij}$  on  $\Delta^{\text{isi}}$  which is later used analogously for  $J_{ij}$ .

In between two spikes of neuron  $j$  only the relaxation dynamics affects the variable  $u_{ij}$ ; thus, we find from Eq. (3)  $u_{ij}(t_2^-) = u_0 + (1 - u_0)u_{ij}(t_1^-)e^{-(\Delta^{\text{isi}}/\nu N)}$ , where  $u_{ij}(t_1^-)$  and  $u_{ij}(t_2^-)$  are the fractions of transmitter available before a spike of neuron  $j$  at times  $t_1$  and  $t_2$ , respectively. At

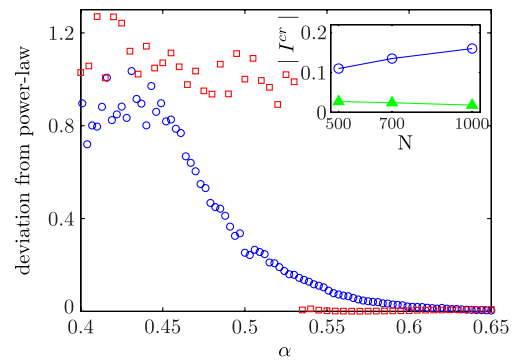


FIG. 2 (color online). Deviation of the avalanche size distribution from a power law for different values of the interaction parameter  $\alpha$ . The deviation is estimated by the minimum of  $\sqrt{\sum_{L=1}^{L_{\text{max}}} [\log P(L, N, \alpha) - \log c_\gamma L^\gamma]^2}$  with respect to  $\gamma$  and  $c_\gamma$ , where  $L_{\text{max}} = N/2$  introduces a cutoff. We checked the unbiasedness of our estimation with the maximum likelihood method. Squares represent the model with both facilitating and depressing synaptic dynamics, circles are for depressing synapses only.  $N = 300$ ,  $\nu = 10$ ,  $u_0 = 0.1$ , and  $I_0 = 7.5$ . The inset shows the length of the critical interval for dynamical synapses (filled symbols) and static synapses (empty symbols)  $N = 500, 700, 1000$ .

stationarity we have  $\langle u_{ij}(t_1^-) \rangle = \langle u_{ij}(t_2^-) \rangle$  and can express  $\langle u_{ij} \rangle$  in terms of  $\langle \Delta^{\text{isi}} \rangle$ ,

$$\langle u_{ij} \rangle = \frac{u_0}{1 - (1 - u_0)e^{-\langle \Delta^{\text{isi}} \rangle / \nu N}} = G_1(\langle \Delta^{\text{isi}} \rangle). \quad (4)$$

Equation (2) provides an analogous expression for  $\langle J_{ij} \rangle$ :

$$\langle J_{ij} \rangle = \frac{\alpha}{u_0} \frac{e^{1/\nu N \langle \Delta^{\text{isi}} \rangle} - 1}{e^{1/\nu N \langle \Delta^{\text{isi}} \rangle} - 1 + \langle u_{ij} \rangle} = G_2(\langle \Delta^{\text{isi}} \rangle). \quad (5)$$

Equations (4) and (5) yield the first part of the self-consistency equation

$$\langle u_{ij} J_{ij} \rangle \approx G_1(\langle \Delta^{\text{isi}} \rangle) G_2(\langle \Delta^{\text{isi}} \rangle) = G(\langle \Delta^{\text{isi}} \rangle). \quad (6)$$

The average synaptic strength  $\langle u_{ij} J_{ij} \rangle$  does not in general equal  $\langle u_{ij} \rangle \langle J_{ij} \rangle$ . This is, however, counterbalanced by the opposite tendencies of the intrinsic dynamics (2) and (3). Direct numerical simulations (Table I) and the further results of this Letter prove that the correlation between  $u_{ij}$  and  $J_{ij}$  can indeed be ignored.

For the dependence of  $\Delta^{\text{isi}}$  on  $\langle u_{ij} J_{ij} \rangle$ , we take into account that the interavalanche interval  $\Delta^{\text{iai}}$  has a geometric distribution  $Q(\Delta^{\text{iai}}) = (I/\theta)[1 - (I/\theta)]^{\Delta^{\text{iai}}}$ . Denoting by  $\kappa_j$  the number of avalanches between two spikes of the neuron  $j$ , the averages of the distributions of interspike and interavalanche intervals are related by  $\langle \Delta^{\text{isi}} \rangle = \langle \kappa \rangle \langle \Delta^{\text{iai}} \rangle$ . The neuronal membrane potentials can be shown to be uniformly distributed between the threshold  $\theta$  and a minimal value  $\epsilon_N$  that is due to the self-interaction of the neurons and the reset. For  $N \rightarrow \infty$  the scaling of the connections implies  $\epsilon_N \rightarrow 0$ . The average interavalanche interval is thus given by  $\langle \Delta^{\text{iai}} \rangle = (\theta - \epsilon_N)/I$ .

In order to determine  $\langle \kappa \rangle$ , we compute the first passage time to threshold  $\theta$ . During the interval  $\Delta^{\text{iai}}$  the neuron receives an external input  $I$  with probability  $1/N$  in a unit time interval (time unit chosen to be  $\tau_s$ ). Therefore, the neuron accumulates an average external input of size  $I \langle \Delta^{\text{iai}} \rangle / N$  during this interval. At avalanches the neuron receives the mean internal input  $\langle u_{ij} J_{ij} \rangle \langle L \rangle$ , where  $\langle L \rangle$  is the mean avalanche size.  $\kappa$  can be expressed by the number of repetitions of interavalanche intervals and the corresponding avalanches, which are required to reach the threshold  $\theta$ .

$$\langle \kappa \rangle = \theta \left( \frac{\langle u_{ij} J_{ij} \rangle \langle L \rangle}{N} + I \frac{\langle \Delta^{\text{iai}} \rangle}{N} \right)^{-1}. \quad (7)$$

The distribution of avalanche sizes is known for a network

TABLE I. Numerical evidence for the independence assumption on the synaptic parameters.  $N = 300$ ,  $u_0 = 0.1$ ,  $\nu = 10$ .

$\alpha$	$\langle u_{ij} \rangle \langle J_{ij} \rangle$	$\langle u_{ij} J_{ij} \rangle$	$ \langle u_{ij} \rangle \langle J_{ij} \rangle - \langle u_{ij} J_{ij} \rangle $
0.40	0.431	0.436	0.005
0.55	0.905	0.911	0.006
0.80	0.957	0.960	0.003

with static synapses of strength  $\alpha_0$  [5]. For dynamical synapses we set  $\alpha_0/N = \langle u_{ij} J_{ij} \rangle$  which allows us to compute  $\langle L \rangle$  as a function of  $\langle u_{ij} J_{ij} \rangle$ :  $\langle L \rangle = \frac{N}{N - (N-1)\langle u_{ij} J_{ij} \rangle}$ .

Combining the previous computations we obtain a relation between the interspike interval and the average synaptic strength.

$$\langle \Delta^{\text{isi}} \rangle = \frac{\theta^2}{I} \left( \frac{\langle u_{ij} J_{ij} \rangle}{N - (N-1)\langle u_{ij} J_{ij} \rangle} + \frac{\theta}{N} \right)^{-1} = F(\langle u_{ij} J_{ij} \rangle). \quad (8)$$

The combination of Eqs. (6) and (8) establishes the self-consistency relation

$$\langle u_{ij} J_{ij} \rangle = G(F[\langle u_{ij} J_{ij} \rangle]), \quad (9)$$

which can be solved graphically for any  $\alpha$ , see Fig. 3. The numerical results (circles in Fig. 3) are in perfect agreement with the analytical solution (9) which demonstrates the validity of the mean-field approximation.

For some values of  $\alpha$  the graphs (6) and (8) intersect in three points, two of which can be shown to be stable, cf. Fig. 4. The unstable solution of the mean-field dynamics is not observed in simulations due to the stochasticity of the dynamics. Thus, if (i)  $\alpha$  is smaller than a lower critical value  $\alpha_c$  then the self-consistency equation (9) has only a single solution. (ii) At  $\alpha = \alpha_c$  a fold bifurcation creates a stable and an unstable branch in addition to the existing stable branch. (iii) Until a second, upper critical value  $\alpha^c$  is reached three solutions coexist, two of which are stable. (iv)  $\alpha = \alpha^c$  is a second bifurcation point where initially stable branch and the unstable branch annihilate such that for (v)  $\alpha > \alpha^c$  only a single solution remains, cf. Fig. 4.

The accuracy of the mean-field approximation in the finite case (Fig. 3) suggests an analysis of the network dynamics in the limit  $N \rightarrow \infty$ . Rewriting Eq. (9)

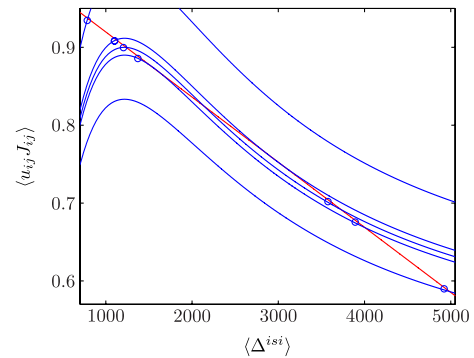


FIG. 3 (color online). Average synaptic strength  $\langle u_{ij} J_{ij} \rangle$  and interspike interval  $\langle \Delta^{\text{isi}} \rangle$  corresponding to Eq. (8) (virtually straight line) and, respectively, Eq. (6) for  $\alpha = 0.5$ ,  $\alpha = \alpha_c$ ,  $\alpha = 0.54$ ,  $\alpha = \alpha^c$ , and  $\alpha = 0.6$  (curved lines, from bottom to top). Circles represent numerical results for a network with matching  $\alpha$  and parameters  $N = 300$ ,  $\nu = 10$ ,  $u_0 = 0.1$ , and  $I_0 = 7.5$ .

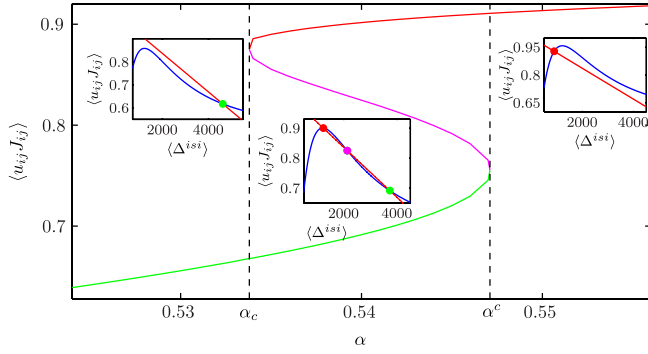


FIG. 4 (color online). Bifurcation diagram representing the solutions of the self-consistency Eq. (9). The effective synaptic strength  $\langle u_{ij}J_{ij} \rangle$  is plotted vs the interaction parameter  $\alpha$ . The insets assign the graphs of Fig. 3 to the corresponding regions by choosing each time a typical  $\alpha$  value.  $N = 300$ ,  $\nu = 10$ ,  $u_0 = 0.1$ , and  $I_0 = 7.5$ .

$$\frac{\alpha}{u_0} \frac{\langle u_{ij} \rangle (1 - e^{-(1/\nu N)\langle \Delta^{isi} \rangle})}{1 - (1 - \langle u_{ij} \rangle) e^{-(1/\nu N)\langle \Delta^{isi} \rangle}} = \frac{N}{N-1} - \frac{I\langle \Delta^{isi} \rangle}{\theta(N-1)} \quad (10)$$

we realize that solutions exist only if  $\Delta^{isi}$  grows linearly in  $N$ . The condition  $\langle \Delta^{isi} \rangle = \text{const}N + o(N)$  implies

$$\alpha > 2\sqrt{u_0(1-u_0)}. \quad (11)$$

This condition is invariant to scaling of the form  $I = I_0 N^{-\mu}$ ,  $\mu > 0$ , and implies that the average synaptic strength approaches unity for large  $N$  which is characteristic for the critical state [5]. In the limit  $N \rightarrow \infty$  the criticality boundary (11) equals the lower boundary of

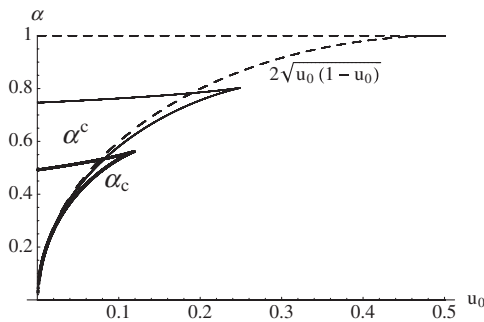


FIG. 5. A cusp is formed in the  $(\alpha, u_0)$  plane by the mergence of the two critical branches  $\alpha_c$  and  $\alpha^c$  into a critical point. The graphs are obtained from Eq. (9) for  $N = 300$  (bold),  $N = 1000$  (semibold), and  $N \rightarrow \infty$  (dashed). For  $N \rightarrow \infty$  the cusp is at  $(\alpha, u_0) = (1, \frac{1}{2})$ . In the interior of the cusp shape, Eq. (9) has three solutions, one of which corresponds to a critical phase and extends also to larger values of  $\alpha$ . The other stable solution is subcritical and exists also below the cusp. At values of  $u_0$  below the critical point, the critical phase is reached by a first-order phase transition for  $N \rightarrow \infty$ , while for higher  $u_0$  values critical behavior is reached by a second-order transition. Further parameters are:  $\nu = 10$ ,  $I_0 = 7.5$ .

the phase coexistence  $\alpha_c$ ; i.e., the phase transition transfers the system into criticality provided the activity of the network is sufficiently high, see Fig. 5. The singular solution remaining above the upper critical value  $\alpha^c$  is as well critical in coincidence with the result in [13].

Our study suggests that critical properties of neuronal dynamics in the brain may be considered as a consequence of the regulatory mechanisms at the level of synaptic connections. By elucidating the relation between the elementary synaptic processes and the network dynamics our mean-field approach revealed a macroscopic bifurcation pattern, which can be verified experimentally, e.g., through predicted hysteresis. Furthermore it may be able to explain observations of up and down states in the prefrontal cortex [14] as well as the discrete changes in synaptic potentiation and depression [15] as a network effect. The relation between neural activity and average synaptic strength, which we derived here, may account for the reported all-or-none behavior.

\*anna@nld.ds.mpg.de

†michael.herrmann@ed.ac.uk

‡geisel@nld.ds.mpg.de

- [1] P. Bak, C. Tang, and K. Wiesenfeld, Phys. Rev. Lett. **59**, 381 (1987).
- [2] B. Gutenberg and C.F. Richter, Ann. Geophys. **9**, 1 (1956).
- [3] V. Frette *et al.*, Nature (London) **379**, 49 (1996).
- [4] H.J.S. Feder and J. Feder, Phys. Rev. Lett. **66**, 2669 (1991).
- [5] C.W. Eurich, M. Herrmann, and U. Ernst, Phys. Rev. E **66**, 066137 (2002); A. Levina, U. Ernst, and J.M. Herrmann, Neurocomputing **70**, 1877 (2007).
- [6] J. M. Beggs and D. Plenz, J. Neurosci. **23**, 11 167 (2003).
- [7] R. A. Legenstein and W. Maass, Neural Networks **20**, 323 (2007).
- [8] C. Haldeman and J. Beggs, Phys. Rev. Lett. **94**, 058101 (2005).
- [9] O. Kinouchi and M. Copelli, Nature Phys. **2**, 348 (2006); D. Chialvo, Nature Phys. **2**, 301 (2006).
- [10] A. M. Thomson and J. Deuchars, Trends Neurosci. **17**, 119 (1994); H. Markram, Y. Wang, and M. Tsodyks, Proc. Natl. Acad. Sci. U.S.A. **95**, 5323 (1998); M. Tsodyks, K. Pawelzik, and H. Markram, Neural Comput. **10**, 821 (1998).
- [11] A. Levina, J. M. Herrmann, and T. Geisel, in *Adv. in NIPS 18* (MIT Press, Cambridge, MA, 2006), pp. 771778.
- [12] H. Markram and M. Tsodyks, Nature (London) **382**, 807 (1996); M. V. Tsodyks and H. Markram, Proc. Natl. Acad. Sci. U.S.A. **94**, 719 (1997).
- [13] A. Levina, J. M. Herrmann, and T. Geisel, Nature Phys. **3**, 857 (2007).
- [14] C. J. Wilson, Prog. Brain Res. **99**, 277 (1993).
- [15] C. C. H. Petersen *et al.*, Proc. Natl. Acad. Sci. U.S.A. **95**, 4732 (1998); D. H. O'Connor, G. M. Wittenberg, and S. S.-H. Wang, Proc. Natl. Acad. Sci. U.S.A. **102**, 9679 (2005).